Published in final edited form as:
Biomaterials. 2010 March ; 31(7): 1666. doi:10.1016/j.biomaterials.2009.11.058.

Dose Effect of Tumor Necrosis Factor-α on *In Vitro* Osteogenic Differentiation of Mesenchymal Stem Cells on Biodegradable Polymeric Microfiber Scaffolds

Paschalia M. Mountziaris, B.S.[1], **Stephanie Tzouanas**[1], and **Antonios G. Mikos, Ph.D.**[1,*]
[1] Department of Bioengineering, Rice University, Houston, TX 77251-1892, USA

Abstract

This study presents a first step in the development of a bone tissue engineering strategy to trigger enhanced osteogenesis by modulating inflammation. This work focused on characterizing the effects of the concentration of a pro-inflammatory cytokine, tumor necrosis factor alpha (TNF-α), on osteogenic differentiation of mesenchymal stem cells (MSCs) grown in a 3D culture system. MSC osteogenic differentiation is typically achieved *in vitro* through a combination of osteogenic supplements that include the anti-inflammatory corticosteroid dexamethasone. Although simple, the use of dexamethasone is not clinically realistic, and also hampers *in vitro* studies of the role of inflammatory mediators in wound healing. In this study, MSCs were pre-treated with dexamethasone to induce osteogenic differentiation, and then cultured in biodegradable electrospun poly(ε-caprolactone) (PCL) scaffolds, which supported continued MSC osteogenic differentiation in the absence of dexamethasone. Continuous delivery of 0.1 ng/mL of recombinant rat TNF-α suppressed osteogenic differentiation of rat MSCs over 16 days, which was likely the result of residual dexamethasone antagonizing TNF-α signaling. Continuous delivery of a higher dose, 5 ng/mL TNF-α, stimulated osteogenic differentiation for a few days, and 50 ng/mL TNF-α resulted in significant mineralized matrix deposition over the course of the study. These findings suggest that the pro-inflammatory cytokine TNF-α stimulates osteogenic differentiation of MSCs, an effect that can be blocked by the presence of anti-inflammatory agents like dexamethasone, with significant implications on the interplay between inflammation and tissue regeneration.

Keywords

cytokine; mesenchymal stem cells; biomineralisation; osteogenesis; bone tissue engineering; inflammation

INTRODUCTION

The limitations of autologous bone grafting and other available surgical reconstructive techniques have led to increased interest in bone tissue engineering, an interdisciplinary strategy to promote healing of large bone defects using bioactive implantable materials. Cells and bioactive factors are incorporated into these scaffolds to provide temporal and spatial cues

*Corresponding author: Professor Antonios G. Mikos, Ph.D., Department of Bioengineering, Rice University, P.O. Box 1892, MS 142, Houston, TX 77251-1892, mikos@rice.edu, Phone: +001-713-348-5355, Fax: +001-713-348-4244.

guiding bone regeneration [1]. However, osteogenesis involves complex molecular signaling and induces significant changes in the expression of several thousand genes [2–4]. To develop an effective tissue engineering strategy for bone regeneration, the key regulators of this process must be identified and incorporated. Informed by cell biology research, efforts to date have focused on inducing bone regeneration via delivery of various bioactive molecules and osteoprogenitor cells. However, recent insight into the critical role of pro-inflammatory cytokines, including tumor necrosis factor alpha (TNF-α), in bone healing has heralded a new direction in the rational design of bone tissue engineering constructs [5,6].

Although the impact of unregulated TNF-α signaling on mature bone in osteoporosis, rheumatoid arthritis, and other pathologies has been studied, the role of TNF-α signaling during bone healing is not well understood [6–10]. Recent studies suggest TNF-α plays an important role in priming bone renewal. Expression of TNF-α rises immediately following bone injury, and is elevated again in later stages of bone regeneration [6,11,12]. Absence of this TNF-α signaling impairs *in vivo* bone fracture healing in a mouse model, delaying endochondral ossification, but it has no effect on skeletal development, suggesting that TNF-α plays a unique role in post-natal osteogenesis [13,14]. We selected TNF-α as a model inflammatory signal for our studies based on its significant impact on *in vivo* bone regeneration.

Our ultimate goal is to develop a novel bone tissue engineering strategy that harnesses inflammation to trigger osteogenesis in large bone defects. However, due to the many gaps in our knowledge regarding the mechanism by which inflammatory signals trigger regeneration, we are first focusing on developing a 3D *in vitro* strategy to better characterize the role of TNF-α on mesenchymal stem cells (MSCs) undergoing osteogenic differentiation. Here we present the results of a study that aimed to establish the effect of TNF-α concentration on osteogenic differentiation of MSCs cultured *in vitro* on biodegradable microfiber scaffolds.

MSCs are a component of the bone marrow stroma, and have the capability to differentiate into various connective tissues, including bone [15]. *In vitro* osteogenic differentiation of MSCs typically requires the addition of dexamethasone [15–17], an anti-inflammatory corticosteroid that is not found in the *in vivo* fracture healing microenvironment and that suppresses *in vivo* bone regeneration [6,18]. Further, dexamethasone is known to antagonize the *in vitro* effects of TNF-α on osteoblasts [19]. Recent efforts have resulted in 3D materials that support *in vitro* differentiation of MSCs without the need for dexamethasone, for instance, by means of a microfiber mesh scaffold coated with pre-generated bone-like extracellular matrix [4,17,20].

In this study we used polymer electrospinning to generate porous mesh scaffolds made of poly (ε-caprolactone) (PCL), a biocompatible and biodegradable polymer [21,22]. By modulating key processing variables, including the PCL concentration, flow rate, collector distance, and applied voltage, PCL microfiber scaffolds with a specific pore size, porosity, and fiber diameter can be reproducibly generated [22]. Scaffold pore size and porosity are key determinants of cell attachment and migration, and also of nutrient transport, all of which affect cell function, proliferation, and differentiation [23–25]. Electrospun PCL fibers with sub-micron diameters have been shown to enhance MSC adhesion and spreading [22]. MSCs were pre-cultured to induce osteogenic differentiation, and then cultured on electrospun PCL microfiber meshes, which we assumed would continue to support MSC osteogenic differentiation even in the absence of dexamethasone.

This study addresses the following questions: (i) What is the impact of continuous TNF-α delivery for 4, 8, and 16 days, and (ii) what is the impact of TNF-α concentration, on osteogenic differentiation of MSCs cultured *in vitro* in 3D biodegradable PCL microfiber scaffolds? MSC-seeded scaffolds were exposed to varying concentrations of TNF-α, which we hypothesized

would enhance osteogenic differentiation in a dose-dependent manner. Our ultimate goal was to determine the impact of TNF-α concentration on *in vitro* 3D osteogenic differentiation of MSCs.

MATERIALS and METHODS

Experimental Design

A design with 6 groups and 3 time points was used to evaluate the impact of TNF-α dose on rat MSC osteogenic differentiation on electrospun poly(ε-caprolactone) (PCL) scaffolds. Low (0.1 ng/mL), medium (5 ng/mL), and high (50 ng/mL) rat TNF-α concentrations were continuously delivered over a 4, 8, or 16-day culture period. Three control groups were included: cell/scaffold constructs cultured without added TNF-α or dexamethasone; a positive control where constructs received dexamethasone (i.e., complete osteogenic media), but did not receive TNF-α; and an acellular control, where cell-free PCL scaffolds were cultured in the absence of both TNF-α and dexamethasone, in order to account for any non-cell-specific scaffold calcium accumulation.

Electrospun Scaffold Generation

The PCL (inherent viscosity = 1.22 dL/g; Lactel, Pelham, AL) had a number-average molecular weight (M_n) = 72,100 ± 1400 Da, weight-average molecular weight (M_w) = 115,000 ± 2200 Da, and polydispersity index (M_w/M_n) of 1.60 ± 0.02, determined via gel permeation chromatography (Phenogel Linear Column with 5 μm particles, Phenomenex, Torrance, CA; Differential Refractometer 410, Waters, Milford, MA) using a calibration curve created from polystyrene standards (Fluka, Switzerland). The PCL was dissolved at 18 w/w% in 5:1 (by vol) chloroform:methanol. This solution was used to generate electrospun meshes of PCL microfibers using a previously decribed apparatus consisting of a syringe pump (Cole Parmer, Vernon Hills, IL), power supply (Gamma High Voltage Research, Osmond Beach, FL), 19 cm diameter copper wire (18 gauge) ring, and a square grounded copper plate (11×11×0.3 cm) [22]. Briefly, 9 mL of PCL solution were loaded into a 10 mL syringe to which a 16 gauge blunt-tip needle (Brico Medical Supplies, Inc., Metuchen, NJ) was attached. The syringe was positioned in the electrospinning apparatus such that the needle tip was 33 cm from a glass collecting plate, placed immediately in front of the grounded copper plate, and 4 cm from the copper ring used to direct the spinning fibers onto the plate. The positive lead from the power supply was split and connected to both the needle tip and the copper ring. A voltage difference of 33 kV was applied and the PCL solution was pumped out of the needle tip at 40 mL/h using the syringe pump. Disks with a diameter of 8 mm were cut from each resulting PCL microfiber mesh using an arch punch (C.S. Osborne & Co., Harrison, NJ). Those disks with thickness 0.90–1.10 mm, as measured using digital micro-calipers (Mitutoyo, Aurora, IL), were used as scaffolds for the study. Two electrospun PCL meshes were required to generate a sufficient number of scaffolds for this study. The meshes were prepared on consecutive days from the same lot of PCL, and using the same electrospinning parameters.

Scaffold Morphology

For scanning electron microscopy (SEM), samples were mounted onto aluminum stubs and sputter-coated with 30 nm of gold. Fiber diameters at the top (n = 45 fibers) and bottom (n = 45 fibers) of each mesh were measured via SEM (FEI Quanta 400 Environmental, Hillsboro, OR) at a 7.31 kV accelerating voltage and 3.0 spot size. The bottom of each mesh was defined as the side adjacent to the glass collecting plate, i.e., the first layer of electrospun PCL microfibers to be deposited. The top of the mesh (the side seeded with MSCs) was thus the final layer of microfibers to be deposited. Several methods were used to minimize bias in the fiber diameter measurements. Scaffolds for SEM imaging (n = 3) were blindly punched from widely separated regions of each PCL mesh. The coordinates of the areas to be imaged on each

scaffold ($n = 3$ on the top, $n = 3$ on the bottom) were established prior to SEM, as was the (previously described) procedure for selecting and measuring fibers ($n = 5$ per field of view) [22].

Scaffold Porosity

The porosity of $n = 50$ scaffolds from each mesh was determined via an established gravimetric analysis protocol [22]. Briefly, the porosity, was calculated based on the apparent density of the scaffold, $\rho_{scaffold}$, and the density of PCL, ρ_{PCL}, according to the equation: $\varepsilon = 1 - \rho_{scaffold}/\rho_{PCL}$. To determine $\rho_{scaffold}$ for each scaffold, mass and volume were measured. To calculate volume, each scaffold was approximated as a cylinder with 8 mm diameter and with height equivalent to the scaffold thickness measured with digital micro-calipers.

Mesenchymal Stem Cell Isolation

Rat MSCs were isolated from the pooled femoral and tibial bone marrow of 8 male syngeneic Fischer 344 rats weighing 150–175 g, according to established methods [4,17]. Bone marrow suspensions were cultured for 7 days in 75 cm^2 flasks using complete osteogenic media, which consists of α-MEM containing 10% v/v fetal bovine serum (Gemini Bio-Products, West Sacramento, CA), 50 mg/L gentamicin, 1.25 μg/mL amphotericin-B (Sigma, St. Louis, MO), as well as 3 osteogenic supplements: 10^{-8} M dexamethasone, 0.01 mM β-glycerophosphate, and 50 μg/mL ascorbic acid (all from Sigma), to induce osteogenic differentiation [4,16]. Culture media was changed on days 1, 3, and 5 to remove non-adherent cells. In this study, the adherent cells are designated as "mesenchymal stem cells," based on the established osteogenic potential of this cell population under appropriate *in vitro* conditions [15,26].

TNF-α Reconstitution and Dilution

Rat TNF-α was used for this study to better model the *in vivo* biology of the rat MSCs, since combining TNF-α from one species (e.g., human TNF-α) with MSCs from another species (e.g., murine MSCs) has been reported to result in TNF-α receptor binding selectivity not seen with native TNF-α [27]. Lyophilized recombinant rat TNF-α (R&D Systems, Minneapolis, MN) was reconstituted on the day of scaffold seeding using sterile phosphate-buffered saline (PBS) containing 0.1 w/w% bovine serum albumin (Sigma), according to the manufacturer's instructions. Aliquots were taken from this 100 ng/μL stock TNF-α solution and further diluted to concentrations of 0.1, 5, and 50 ng/μL. All reconstituted TNF-α solutions were split into aliquots, to minimize the number of freeze/thaw cycles, and stored at −20°C in a manual defrost freezer, according to the manufacturer's instructions. For experiments, 4 μL of diluted solution were added to 4 mL of media used for construct culture, resulting in the desired experimental group concentrations of 0.1, 5, and 50 ng/mL TNF-α.

Scaffold Preparation

Electrospun PCL scaffolds were prepared for MSC seeding according to established protocols [22]. The scaffolds were sterilized via exposure to ethylene oxide gas for 14h, and then passed through a decreasing ethanol gradient (from 100% to 70%) to expel air from the scaffold pores. Centrifugation was used to ensure complete prewetting. The ethanol was exchanged with sterile milliQ water, and the scaffolds were then immersed in dexamethasone-free osteogenic media and left in an incubator overnight. Prior to MSC seeding, the scaffolds were press-fit into seeding cassettes and placed into 6-well plates (1 cassette/well). Ultra-low attachment 6-well plates (Corning Incorporated Life Sciences, Lowell, MA), consisting of a neutral, hydrophilic hydrogel covalently bound to a polystyrene well-plate, were used based on the results of a pilot study indicating increased retention of MSCs on electrospun PCL scaffolds (i.e., reduced adhesion of MSCs to the bottom of the well) without any impact on MSC osteogenic differentiation.

Scaffold Seeding and Culture

Nearly confluent MSCs were detached from the cell culture flasks with 0.25% trypsin/EDTA (Sigma, St. Louis, MO), counted with a hemocytometer, centrifuged, and resuspended at 1.25 million cells/mL in dexamethasone-free osteogenic media, which is identical in composition to complete osteogenic media, except that it lacks dexamethasone. Although dexamethasone is typically used as an osteogenic supplement *in vitro* [16,17], it was not included in the media used for MSC/scaffold culture because this portion of the study involved TNF-α supplementation, and dexamethasone has been shown to antagonize the *in vitro* effects of TNF-α on osteoblasts [19]. For seeding, 200 μL of the resuspended MSCs were added drop-wise to each scaffold, which had already been press-fit into a seeding cassette and placed in a 6-well plate (Corning), as detailed above. MSCs were allowed to attach to the scaffolds for 4h, and then each well was filled with dexamethasone-free media as well as supplemental TNF-α or dexamethasone, as appropriate. After 24h, cell/scaffold constructs (n = 15 per group) were transferred to new ultra-low attachment 6-well plates (1 construct/well). 4 mL of dexamethasone-free media were added to each well, and relevant groups also received supplemental TNF-α (0.1, 5, or 50 ng/mL per well) or dexamethasone (10^{-8} M/well). Thereafter, media and supplements were changed every two days for a total of 4, 8, or 16 days of culture.

Cellularity Measurement

Construct cellularity was quantified according to an established protocol [17]. At each timepoint, n = 4 constructs from each group were rinsed twice with PBS and placed in 1 mL of sterile milliQ water. The cells were lysed and cell contents were extracted with 3 freeze/thaw/sonication cycles (10 min at −80°C, 10 min at 37°C, 10 min sonication). The dsDNA content of each resulting solution was quantified using the fluorometric PicoGreen assay (Molecular Probes, Eugene, OR) with an excitation wavelength of 490 nm and an emission wavelength of 520 nm, as detailed elsewhere [17]. Samples and dsDNA standards were run in triplicate. The results were converted to cells per construct using the previously established DNA content of rat MSCs [17].

Alkaline Phosphatase Activity Assay

Alkaline phosphatase (ALP) activity of MSC-seeded scaffolds was used as an early marker of osteogenic differentiation [17]. An established colorimetric assay was used to quantify ALP activity based on the rate of conversion of a colorless substrate, *p*-nitrophenyl phosphate disodium salt hexahydrate (Sigma), to a yellow product, *p*-nitrophenol [17]. The assay was prepared in a 96-well plate using aliquots of the same cell lysate used to measure cellularity, according to an established protocol [17]. Samples were run in triplicate, and diluted to fall within the range of the *p*-nitrophenol standards. After 1h incubation at 37°C, the reaction was stopped with 0.3 M NaOH and the absorbance at 405 nm was measured with a plate reader. ALP activity was normalized to construct cellularity [17].

Calcium Content Assay

The acid-soluble calcium content of MSC-seeded scaffolds was used to quantify mineralized matrix deposition, which is a late-stage marker of osteogenic differentiation [17]. An established colorimetric assay was used to quantify calcium content based on the color change that occurs when a calcium chelating agent (Arsenazo III, Diagnostic Chemicals, Oxford, CT) binds to free calcium in an acid solution. Prior to the assay, each construct was removed from the aqueous cell lysate, immersed in 1 mL 1 N acetic acid, and left on a shaker table at 200 rpm overnight to dissolve matrix-bound calcium. The assay was prepared in a 96-well plate as previously described, and absorbance at 650 nm was read after a 10 min incubation [17]. Samples were run in triplicate and diluted to fall within the range of the $CaCl_2$ standards.

Histological Sample Preparation

At each timepoint, $n = 1$ construct from each group was rinsed twice with PBS and fixed overnight in 5 mL of 10% buffered formalin phosphate. Constructs were then passed through an ascending (70% to 100%) ethanol gradient and stored in 100% ethanol at 4°C. Prior to sectioning, each construct was cut in half using a razor blade, so that cross-sectional images could be obtained. Half was returned to storage in 100% ethanol and the other half was embedded in HistoPrep frozen tissue embedding media (Fisher Scientific, Pittsburgh, PA). Frozen 5 μm thick sections were cut using a cryotome (CM1850, Leica Microsystems, Bannockburn, IL) and mounted on Superfrost Plus glass slides (Fisher Scientific). The slides were incubated at 45°C on a slide warmer for 4–5 days for optimal section adhesion.

Histological Staining and Imaging

To visualize the distribution of mineralized matrix and cells within each construct, sections were rehydrated with water for 1 min and then immersed in von Kossa stain (5% w/w silver nitrate in milliQ water) under UV for 30 min. Residual stain was removed by gentle drop-wise rinsing with water followed by 95% ethanol. Sections were then counter-stained with alcoholic eosin Y (Sigma) for 3 min. Residual eosin was removed by gentle drop-wise rinsing with 95% ethanol. Once dry, stained slides were imaged with a light microscope (Eclipse E600, Nikon, Melville, NY) using an attached video camera (3CCD Color Video Camera DXC-950P, Sony, Park Ridge, NJ) and computer. Light microscope images were calibrated using the standard two-image method to correct for differences in background lighting and in dark-current effects in the detector [28].

Statistical Analysis

Fiber diameters and porosities are reported as mean ± standard deviation for $n = 45$ fibers and $n = 50$ scaffolds, respectively. The average fiber diameter of the top and bottom of each PCL microfiber mesh, along with the average porosity, were compared using a Student's t-test for two independent samples with equal variance ($\alpha = 0.05$) after performing an F-test to validate the assumption of equal variance at 95% confidence. Cellularity, ALP activity, and calcium assay results are reported as mean ± standard deviation for $n = 4$ constructs. Statistical differences in cellularity, ALP activity, and calcium content amongst groups at each time point, and also within each group over time, were analyzed at 95% confidence using one-way analysis of variance. Multiple pair-wise comparisons were made using the Bonferroni post-hoc analysis method at 95% confidence.

RESULTS

The two electrospun PCL microfiber meshes fabricated for this study had statistically equivalent mean fiber diameters ($p > 0.05$), as shown in Table 1. Although the average porosities of the two meshes were statistically different ($p < 0.05$), the magnitude of the difference was quite small (77.8 ± 2.8% vs. 79.5 ± 3.1%), and so the two meshes were used to generate the PCL scaffolds for this study. Equal numbers of scaffolds were randomly selected from each mesh. Figure 1 shows representative scaffold morphology obtained via SEM at varying magnifications.

Figure 2 depicts the number of cells in the constructs after 4, 8, and 16 days of culture. Most groups had similar cellularity at each timepoint, with a few exceptions. The acellular control ("Acellular") had nearly zero cells/scaffold at all timepoints, as expected. The cellularity of the positive control group ("0 ng/mL TNF +dex") peaked at the earliest timepoint (day 4), at a value significantly higher than the number of cells on the experimental constructs ($p < 0.05$). The number of cells on the positive control constructs subsequently declined (values at all three timepoints differ, $p < 0.05$), such that this group had significantly fewer cells than the other

groups at day 16 ($p < 0.05$). The negative control group ("0 ng/mL TNF") followed a similar trend, although no statistical differences were detected between timepoints ($p > 0.05$). In contrast, the lowest dose of TNF-α ("0.1 ng/mL TNF") induced proliferation resulting in a monotonic increase in cellularity (values at all three timepoints differ, $p < 0.05$), with cell numbers for this group exceeding those of all others on days 8 and 16 ($p < 0.05$). The highest dose of TNF-α ("50 ng/mL TNF") also induced proliferation, but cellularity peaked at day 8 and then declined (day 4 and day 16 values both differ from day 8, $p < 0.05$). The middle dose of TNF-α ("5 ng/mL TNF") followed a similar trend, with an apparent peak at day 8 and subsequent plateau, but no statistical differences were detected between timepoints ($p > 0.05$).

Figure 3 shows the ALP activity of the constructs on a per cell basis. Dexamethasone induced ALP activity, such that the 0 ng/mL TNF +dex positive control had significantly higher values than all other groups at each timepoint ($p < 0.05$), and showed an increasing trend throughout the study (all timepoints different, $p < 0.05$). Unlike the positive control, the ALP activity of the 0 ng/mL TNF negative control did not change throughout the study (all timepoints similar, $p > 0.05$), although it did appear to be declining by day 16. In contrast, supplementation with TNF-α greatly reduced ALP activity on a per cell basis. The experimental groups had significantly lower ALP activity than both of the MSC-seeded control groups at all timepoints ($p < 0.05$). This suppression appeared dose-dependent on day 4 since 0.1 ng/mL TNF had higher ALP activity than 50 ng/mL TNF ($p < 0.05$), and the value for 5 ng/mL TNF fell between these two. Although the ALP activity of 0.1 ng/mL TNF remained higher than that of the other two experimental groups at all timepoints ($p < 0.05$), these groups showed divergent trends over time. The ALP activity of 0.1 ng/mL TNF peaked at day 8 (all timepoints differ, $p < 0.05$), while 5 ng/mL TNF and 50 ng/mL TNF had monotonically decreasing ALP activity (in each group, all timepoints differ, $p < 0.05$), that was indistinguishable from the acellular group by day 16 ($p > 0.05$). As expected, the acellular control had nearly zero ALP activity at all timepoints.

Figure 4 illustrates the acid-soluble calcium content of the constructs after 4, 8, and 16 days of culture. The calcium content of all groups, with the exception of the acellular control, monotonically increased over time. Dexamethasone induced the greatest amount of overall calcium deposition, such that the 0 ng/mL TNF +dex positive control had significantly higher values than all other groups on days 8 and 16 ($p < 0.05$), and showed an increasing trend throughout the study (all timepoints different, $p < 0.05$). TNF-α triggered early mineralized matrix deposition in a dose-dependent manner, such that 5 ng/mL TNF had significantly more calcium on day 4 than the control groups and 0.1 ng/mL TNF ($p < 0.05$), and 50 ng/mL TNF had even more calcium ($p < 0.05$). After day 4, the rate at which calcium was deposited in these constructs declined, while the calcium deposition rate of the controls increased. By day 8, the negative control (0 ng/mL TNF) and 50 ng/mL TNF constructs had similar calcium content ($p > 0.05$), and continued to deposit similar amounts of calcium through day 16 ($p > 0.05$). On both days 8 and 16, the calcium content of 0 ng/mL TNF and 50 ng/mL TNF significantly exceeded that of the other two experimental groups ($p < 0.05$). In fact, the lower doses of TNF-α almost completely suppressed calcium deposition. The mineralized matrix deposition rate of the 5 ng/mL TNF constructs fell to zero after day 4, so that essentially no further calcium was deposited over the course of the study. The calcium content of the 0.1 ng/mL TNF constructs also plateaued; it increased ($p < 0.05$) from a near-zero level on day 4 to a level equivalent to the 5 ng/mL TNF constructs on day 8. Neither group showed any further calcium deposition on day 16 ($p > 0.05$).

The results of the cellularity and calcium content assays were confirmed qualitatively through histological analysis, shown in Figure 5. Sections were stained with von Kossa, which stains mineralized extracellular matrix black, and counter-stained with eosin, which dyes cytoplasmic material and organic matrix components (e.g., collagen) reddish-pink. The highest density of

mineralized matrix was observed at the top of the scaffolds, visible as black deposits of varying widths and ~40 μm thickness (blue arrows in Fig. 5). Consistent with the calcium assay data (Fig. 4), 50 ng/mL TNF sections stained the darkest with von Kossa on day 4, while 0 ng/mL TNF +dex was the darkest-staining group on days 8 and 16 (Fig. 5). The presence of the black-stained mineralized matrix made it difficult to discern the cells in sections with high calcium because the matrix was co-localized with cells.

In general, the highest density of cells was observed at the top of the scaffolds. At the earliest timepoint, when the calcium content of all groups was at its lowest, a 5-10 μm thick pink-stained layer of cells and non-mineralized matrix was visible at the top of each section (indicated by yellow arrows), except for the acellular construct (Fig. 5). Consistent with cellularity (Fig. 2) and calcium measurements (Fig. 4), a very thick (~30 μm) reddish-pink layer of cells and (mostly non-mineralized) matrix was observed on the top surface of the 0.1 ng/mL TNF sections on days 8 and 16 (see representative images in Fig. 5). Cells infiltrated 200–500 μm into each microfiber scaffold; these lower-density collections of cells gave the upper ~200 μm of the section a grayish tint (e.g., day 8 image of 0 ng/mL TNF in Fig. 5), and/or appeared as grayish threads and speckles amidst the PCL fibers (e.g., yellow arrows in lower half of day 16 image of 0 ng/mL TNF in Fig. 5). The grayish color of these features is an artifact of the low magnification (10×) used to capture the images in Figure 5. At higher magnification (not shown), these structures were tinted pink, as expected for eosin-stained cells. Mineralized matrix was also deposited on PCL fibers 200–500 μm below the surface, consistent with the depth of cell infiltration. This was particularly evident when comparing the lower portions of the stained sections (e.g., day 16 images of 0 ng/mL TNF +dex, 0 ng/mL TNF, and Acellular in Fig. 5).

DISCUSSION

The goal of this study was to determine the effect of TNF-α dose on MSC osteogenic differentiation in a 3D biodegradable microfiber mesh scaffold. The lowest TNF-α concentration (0.1 ng/mL) for this study was selected because it approximates the physiologic level of TNF-α measured in wound fluid from patients with severe bone injuries [29]. The medium (5 ng/mL) and high TNF-α concentrations (50 ng/mL) were selected based on previous studies demonstrating differential effects on the 2D osteogenic differentiation of MSCs [8,9, 30]. We found that continuous delivery of a low dose (0.1 ng/mL) of recombinant rat TNF-α suppressed osteogenic differentiation of rat MSCs over 16 days. In contrast, continuous delivery of a higher dose, 5 ng/mL TNF-α, stimulated osteogenic differentiation for a few days, and 50 ng/mL TNF-α resulted in significant mineralized matrix deposition over the course of the study. Our findings suggest that TNF-α stimulates osteogenic differentiation of MSCs, and that this effect can be antagonized by signaling resulting from pre-culture with the anti-inflammatory agent dexamethasone.

An important feature of this study is the use of TNF-α and MSCs from the same species. Recombinant rat TNF-α was used to better model the *in vivo* biology, since the MSCs were from a rat source. Rats were selected in anticipation of future *in vivo* implantation studies to evaluate bone regeneration using an established rat critical size cranial defect model [31]. To our knowledge, no other studies have reported on the ALP activity and mineralized matrix deposition of rat MSCs treated with rat TNF-α *in vitro* either in 2D or 3D culture. Several previous studies with rat osteoprogenitors have inter-mingled species; for instance, fetal rat calvarial osteoblasts were treated with recombinant human TNF-α, resulting in decreased calcium deposition when TNF-α was given during the first two weeks of culture, and no effect if TNF-α administration began thereafter [32,33]. However, inter-species variability in TNF-α is significant, as shown rigorously for humans and mice. Human TNF-α selectively binds to the type 1 TNF receptor on murine MSCs, while murine TNF-α has equal affinity for both type

1 and 2 TNF-α receptors [27]. Thus, it is difficult to use the results of these studies to better understand the *in vivo* impact of TNF-α. Additionally, studies using MSCs and TNF-α from the same species have shown divergent effects. Human MSCs treated *in vitro* with human TNF-α for 14-21d showed increased ALP activity and calcium deposition [8,10], while recombinant murine TNF-α (also delivered for 14-21d) suppressed ALP activity and mineralized matrix deposition of murine MSCs [9,34]. This suggests that species physiology affected our osteogenic marker results.

Our results indicate that unmodified electrospun PCL microfiber meshes support 3D osteogenic differentiation of MSCs. This was not seen in similar *in vitro* studies with titanium microfiber meshes, where scaffolds required a pregenerated bone-like mineralized matrix coating in order to support *in vitro* rat MSC osteogenic differentiation under static conditions, particularly in the absence of dexamethasone [17]. In this study, the calcium per construct achieved in the 0 ng/mL TNF +dex positive control constructs after 16 days (Fig. 4) far exceeds the values reported for MSC-seeded titanium microfiber meshes under similar *in vitro* conditions (644.5 ± 14.9 μg vs. 10–20 μg), and is similar to the net calcium deposition achieved when the titanium microfibers were coated with pregenerated bone-like matrix [17]. Similarly, the 407.6 ± 14.1 μg of calcium deposited after 16 days in the absence of dexamethasone (0 ng/mL TNF values in Fig. 4) exceeds that for both unmodified (~0 μg) and bone-like matrix coated (213.2 ± 13.6 μg) titanium microfiber constructs [17]. Several potential explanations for these findings exist. The batch of MSCs used for this study may have had inherently higher capacity for mineralized matrix deposition. This is a less likely explanation, however, since the MSCs from 5 or more rats were pooled to reduce such variability. Additionally, similar high calcium values have been achieved in pilot studies using MSC-seeded PCL scaffolds (results not shown). The hydrophobicity of the PCL microfibers may have played a role by promoting protein adsorption and subsequent cell adhesion, which may have enhanced osteogenic differentiation. PCL was selected for the generation of electrospun microfiber scaffolds because of its biocompatibility and very slow degradation rate, such that scaffolds implanted *in vivo* as a component of a future bone tissue engineering strategy would promote tissue ingrowth and provide structural support within a bone defect, and then later degrade to allow for remodeling of the regenerated bone [22,25]. The variation in fiber size inherent to the generation of electrospun PCL meshes may have been beneficial, compared to the relatively uniform prefabricated titanium meshes. SEM indicated that although largely comprised of ~10 μm diameter fibers, the PCL meshes also contained some smaller fibers (Fig. 1a,b). Electrospun PCL fibers with sub-micron diameters have been shown to enhance rat MSC adhesion and spreading [22]. The results of this study indicate that electrospun PCL microfiber meshes are promising candidates as components of 3D *in vitro* culture systems to better understand the role of inflammatory mediators in MSC osteogenic differentiation.

We capitalized on this finding to culture MSCs in the absence of dexamethasone, which was particularly important as this anti-inflammatory corticosteroid blocks the *in vitro* effects of TNF-α on osteoblasts [19]. Corticosteroids, including dexamethasone, interfere with intracellular TNF-α signaling mainly by binding to and inactivating nuclear factor-κB (NF-κB), a transcription factor [18]. TNF-α binding to cell-surface receptors activates NF-κB, which travels from the cell cytoplasm to the nucleus, binds to DNA, and activates specific genes. Antagonizing NF-κB blocks many effects of TNF-α on cells [18]. Unlike TNF-α, corticosteroids are not found in the *in vivo* fracture healing microenvironment and have been shown to suppress *in vivo* bone regeneration [6,18]. Thus, the exclusion of dexamethasone from the culture media of all but the positive control group had the benefit of making the 3D culture system described herein a better approximation of *in vivo* bone biology.

However, dexamethasone is commonly used for *in vitro* MSC culture, in combination with ascorbic acid and β-glycerophosphate, due to the resulting significant stimulation of osteogenic

markers like ALP activity and mineralized matrix deposition [15–17]. In this study, all three of these supplements were provided to the rat MSCs during the 2D pre-culture expansion period based on previous reports that dexamethasone is necessary to initiate *in vitro* osteogenic differentiation of rat MSCs [15,17]. Dexamethasone supplementation was discontinued once the MSCs were seeded onto the biodegradable PCL microfiber scaffolds, i.e., during the portion of the study involving TNF-α supplementation. The only exception was the 0 ng/mL TNF +dex positive control group, which received continuous dexamethasone supplementation and as a result showed elevated markers of osteogenic differentiation, with the highest level of ALP activity throughout the study ($p < 0.05$; Fig. 3) and the highest level of calcium deposition on days 8 and 16 ($p < 0.05$; Fig. 4).

The decrease in cellularity over time observed in the 0 ng/mL TNF +dex positive control (Fig. 2; values at all three timepoints differ, $p < 0.05$) is consistent with our previous experience with rat MSC osteogenic differentiation on titanium meshes (20 μm fiber diameter) [17] and starch-PCL blend (180 μm fiber diameter) scaffolds [25]. Two possible explanations for this decline in measured cellularity over time have been reported. One possibility is that it is an artifact of late-stage osteogenic differentiation of MSCs, which results in increased deposition of mineralized matrix that traps DNA and prevents its detection [17]. The 0 ng/mL TNF +dex constructs exhibited high levels of calcium deposition on days 8 and 16 (Fig. 4), a trend confirmed by von Kossa staining (Fig. 5). Histology also indicated that calcified matrix co-localized with cells and the (eosin-stained) cell content of the 0 ng/mL +dex constructs appeared to increase over time, particularly from days 4 to 8 (Fig. 5), suggesting that complete DNA detection may have been impaired by the high mineralized matrix content of these constructs. This mechanism could also be applied to the subtly declining cell counts seen in the dexamethasone-free negative control (Fig. 2; non-significant decreasing trend for 0 ng/mL TNF constructs, $p > 0.05$), and also to the 50 ng/mL TNF group, where measured cellularity declined significantly from day 8 to day 16 (Fig. 2; $p < 0.05$); this finding was not seen with the other two doses of TNF-α. At the same time, calcium content of the 0 ng/mL TNF and 50 ng/mL TNF constructs increased significantly (Fig. 4; all three timepoints differ within each group, $p < 0.05$) and greatly exceeded that for the other two TNF-α doses on days 8 and 16 (Fig. 4; $p < 0.05$).

Another possible explanation for the decrease in cellularity over time observed in the 0 ng/mL TNF +dex positive control (Fig. 2; values at all three timepoints differ, $p < 0.05$) is a direct effect of dexamethasone, which is known to support MSC proliferation in some cases and inhibit it in others. Factors influencing this effect include dexamethasone dose and duration, as well as MSC species and stage of osteogenic differentiation [15]. Under this theory, the subtle decline in cellularity seen for the 0 ng/mL TNF (Fig. 2; non-significant decreasing trend, $p > 0.05$) and 50 ng/mL groups (Fig. 2; significant decline from days 8–16, $p < 0.05$) would be attributable to end-stage osteogenic differentiation of the MSCs, associated with cessation of cell proliferation, decreased early-stage markers (in this study, ALP activity shown in Fig. 3; non-significant decreasing trend for 0 ng/mL TNF, $p > 0.05$, and significant decreasing trend for 50 ng/mL TNF, $p < 0.05$), and elevated late-stage markers (here, mineralized matrix deposition in Fig. 4; significant increasing trends for 0 ng/mL TNF and 50 ng/mL TNF, $p < 0.05$). In contrast, the substantial decrease in cell content of the 0 ng/mL TNF +dex constructs (Fig. 2; cellularity lower than all other groups except acellular on day 16, $p < 0.05$) would be the combined result of terminal MSC differentiation into osteoblasts and a direct effect of dexamethasone on cellularity. Further studies are required to distinguish between these two possibilities.

Overall, no adverse effect of 0.1 – 50 ng/mL TNF-α on cell viability was seen over the course of 16 days, consistent with recent reports for 2D *in vitro* MSC cultures in dexamethasone-free osteogenic media [8,10]. Although cell counts in the experimental constructs were lower than

in the controls on day 4 ($p < 0.05$), this difference was no longer present by day 8 (Fig. 2). The monotonic increase in cellularity over time for 0.1 ng/mL TNF constructs (Fig. 2; values at all three timepoints differ, $p < 0.05$) is consistent with proliferation recently reported for human MSCs encapsulated in 3D poly(ethylene glycol)-based hydrogels and exposed to recombinant human TNF-α for 14 days in the presence of dexamethasone [5]. This increase in proliferation was suggested to indicate that TNF-α inhibits osteogenic differentiation of human MSCs, particularly when combined with data indicating that TNF-α suppressed ALP activity of human MSCs in the hydrogels [5]. However, it is likely that these published results reflect the combined, opposing effects of TNF-α and dexamethasone delivery.

In this study, the divergent effects of low and high doses of TNF-α on markers of MSC osteogenic differentiation likely arose from the relative balance between dexamethasone- and TNF-α-related signaling early in 3D culture. Our results for the 0.1 ng/mL TNF constructs suggest that TNF-α inhibited osteogenic differentiation, but the data for the 50 ng/mL TNF group suggest the opposite. Previous studies have reported one result or the other, but never a combination of the two findings as in our case. The most likely explanation is a residual effect of the dexamethasone that was used as a supplement during the MSC *in vitro* pre-culture period. Corticosteroids, including dexamethasone, are internalized by cells and bind to an intracellular receptor, so the *in vitro* effects of dexamethasone can persist for up to 2 weeks after its removal from the environment [15,18]. Thus, despite the separation in the delivery of dexamethasone and TNF-α during MSC culture, our results suggest that intracellular signals arising from the two agents interacted and impacted MSC osteogenic differentiation.

The 7-day pre-culture period used for the rat MSCs in this study typically results in committed osteoprogenitor cells that are not yet mature osteoblasts [35]. By day 4 of our study, TNF-α had reduced ALP activity (Fig. 3; $p < 0.05$) and increased mineralized matrix deposition (Fig. 4; $p < 0.05$) in a dose dependent manner. However, this effect was not maintained over the course of 16 days for lower doses of TNF-α. The ALP and calcium data for the 0.1 ng/mL TNF group indicate suppressed osteogenic differentiation over the course of 16 days. Both osteogenic markers were significantly lower than the values for positive and negative control groups throughout the study (ALP activity suppressed, $p < 0.05$ in Fig. 3; calcium content reduced, $p < 0.05$ in Fig. 4). When considered together with the cellularity data, where the 0.1 ng/mL constructs showed a monotonic increase in cell content (Fig. 2; all three timepoints differ, $p < 0.05$), these data are consistent with previous reports of simultaneous delivery of dexamethasone and TNF-α, which stimulated an immature, proliferative phenotype in human MSCs [5]. In contrast, the highest dose of TNF-α had the opposite effect on MSCs; cell content remained fairly constant throughout the study (Fig. 2), while mineralized matrix content increased monotonically (Fig. 4; all three timepoints differ, $p < 0.05$), consistent with progression towards terminal osteogenic differentiation and with previous reports of human MSCs treated with human TNF-α in the absence of dexamethasone [8,10]. The 5 ng/mL TNF constructs showed a similar pattern, with constant cellularity (Fig. 2), declining ALP activity (Fig. 3; all three timepoints differ, $p < 0.05$), and significantly elevated mineralized matrix content on day 4 (Fig. 4; exceeds all groups except 50 ng/mL TNF, $p < 0.05$). However, mineralized matrix deposition appeared to halt after day 4 for this group, so that the values on days 8 and 16 were equivalent to those of the 0.1 ng/mL TNF constructs (Fig. 4; $p > 0.05$). Thus, the lowest dose of TNF-α may have only been sufficient to cancel out the effects of dexamethasone, halting MSC osteogenic differentiation, while the higher doses were able to also exert a TNF-α-related effect on the MSCs, resulting in increased calcium deposition.

Our findings of increased mineralized matrix deposition triggered by TNF-α delivery in the absence of dexamethasone are supported by several studies in a variety of cell types. TNF-α delivered for 28d in the absence of dexamethasone promoted odontoblastic differentiation and increased mineralized matrix deposition of dental pulp cells [36]. Increased calcium deposition

in vitro has also been reported for vascular-derived cells treated with TNF-α in the absence of dexamethasone [37]. In addition, human MSCs treated *in vitro* with human TNF-α for 14-21d showed increased calcium deposition in the absence of dexamethasone [8,10]. However, a similar study in murine MSCs indicated that recombinant murine TNF-α suppressed ALP activity and mineralized matrix deposition regardless of the presence of dexamethasone [9, 34], which serves as a reminder that species physiology also impacted our results. Overall, our results suggest that the pro-inflammatory cytokine TNF-α stimulates *in vitro* mineralized matrix deposition by MSCs, a late-stage marker of osteogenic differentiation, and that this effect is likely antagonized by the anti-inflammatory agent dexamethasone. Future studies will expand on this exciting finding to establish the optimal time period for delivery and, ultimately, whether TNF-α can be used as a more physiologically realistic replacement to the traditional osteogenic supplement dexamethasone.

CONCLUSIONS

This study demonstrated that the pro-inflammatory cytokine TNF-α stimulates mineralized matrix deposition, a late stage marker of osteogenic differentiation, when delivered continuously to MSCs cultured in 3D electrospun PCL microfiber meshes. By day 4 of our study, TNF-α had reduced ALP activity, an early marker of osteogenic differentiation, and increased mineralized matrix deposition in a dose dependent manner. However, this effect was not maintained over the course of 16 days for lower doses of TNF-α. Continuous delivery of 0.1 ng/mL of TNF-α induced proliferation and suppressed osteogenic markers in MSCs over 16 days, an effect that likely arose from the antagonism of TNF-α by anti-inflammatory signaling induced by the corticosteroid dexamethasone, which was used as an osteogenic supplement during *in vitro* MSC pre-culture. In contrast, continuous delivery of a higher dose, 5 ng/mL TNF-α, stimulated osteogenic differentiation for a few days, and 50 ng/mL TNF-α resulted in significant mineralized matrix deposition over the course of the study. This suggests that the lowest dose of TNF-α was only sufficient to cancel out the effects of dexamethasone, halting MSC osteogenic differentiation, while the higher doses were able to also exert a TNF-α-related effect on the MSCs, resulting in increased calcium deposition. Based on these results we conclude that TNF-α stimulates osteogenic differentiation, and that its effects on MSCs can be blocked by the presence of anti-inflammatory agents like dexamethasone.

Acknowledgments

We acknowledge financial support by the National Institutes of Health (R01 DE17441). PMM is supported by a training fellowship from the Keck Center Nanobiology Training Program of the Gulf Coast Consortia (NIH Grant No. 5 T90 DK070121-04).

Abbreviations

ALP	alkaline phosphatase
+dex	supplemented with dexamethasone
MSCs	mesenchymal stem cells
NF-κB	nuclear factor-κB
PBS	phosphate-buffered saline
PCL	poly(ε-caprolactone)
SEM	scanning electron microscopy
TNF-α	tumor necrosis factor alpha

UV ultraviolet light

References

1. Ingber DE, Levin M. What lies at the interface of regenerative medicine and developmental biology. Development 2007;134:2541–2547. [PubMed: 17553905]
2. Rundle CH, Wang H, Yu H, Chadwick RB, Davis EI, Wegedal JE, et al. Microarray analysis of gene expression during the inflammation and endochondral bone formation stages of rat femur fracture repair. Bone 2006;38:521–529. [PubMed: 16321582]
3. Hecht J, Kuhl H, Haas SA, Bauer S, Poustka AJ, Lienau J, et al. Gene identification and analysis of transcripts differentially regulated in fracture healing by EST sequencing in the domestic sheep. BMC Genomics 2006;7:172. [PubMed: 16822315]
4. Pham QP, Kasper FK, Baggett LS, Raphael RM, Jansen JA, Mikos AG. The influence of the in vitro generated bone-like extracellular matrix on osteoblastic gene expression of marrow stromal cells. Biomaterials 2008;29(18):2729–2739. [PubMed: 18367245]
5. Lin C-C, Metters AT, Anseth KS. Functional PEG-peptide hydrogels to modulate local inflammation induced by the pro-inflammatory cytokine TNF[alpha]. Biomaterials 2009;30(28):4907–4914. [PubMed: 19560813]
6. Mountziaris PM, Mikos AG. Modulation of the inflammatory response for enhanced bone tissue regeneration. Tissue Eng Part B Rev 2008;14(2):179–186. [PubMed: 18544015]
7. Guo R, Yamashita M, Zhang Q, Zhou Q, Chen D, Reynolds DG, et al. Ubiquitin ligase smurf1 mediates tumor necrosis factor-induced systemic bone loss by promoting proteasomal degradation of bone morphogenetic signaling proteins. J Biol Chem 2008;283(34):23084–23092. [PubMed: 18567580]
8. Ding J, Ghali O, Lencel P, Broux O, Chauveau C, Devedjian JC, et al. TNF-[alpha] and IL-1[beta] inhibit RUNX2 and collagen expression but increase alkaline phosphatase activity and mineralization in human mesenchymal stem cells. Life Sci 2009;84(15–16):499–504. [PubMed: 19302812]
9. Lacey DC, Simmons PJ, Graves SE, Hamilton JA. Proinflammatory cytokines inhibit osteogenic differentiation from stem cells: implications for bone repair during inflammation. Osteoarthritis Cartilage 2009;17(6):735–742. [PubMed: 19136283]
10. Hess K, Ushmorov A, Fiedler J, Brenner RE, Wirth T. TNF[alpha] promotes osteogenic differentiation of human mesenchymal stem cells by triggering the NF-[kappa]B signaling pathway. Bone 2009;45 (2):367–376. [PubMed: 19414075]
11. Kon T, Cho T-J, Aizawa T, Yamazaki M, Nooh N, Graves DT, et al. Expression of osteoprotegerin, receptor activator of NF-κB ligand (osteoprotegrin ligand) and related pro-inflammatory cytokines during fracture healing. J Bone Miner Res 2001;16(6):1004–1014. [PubMed: 11393777]
12. Gerstenfeld LC, Cullinane DM, Barnes GL, Graves DT, Einhorn TA. Fracture healing as a post-natal developmental process: Molecular, spatial, and temporal aspects of its regulation. J Cell Biochem 2003;88:873–884. [PubMed: 12616527]
13. Gerstenfeld LC, Cho T-J, Kon T, Aizawa T, Tsay A, Fitch J, et al. Impaired fracture healing in the absence of TNF-α signaling: The role of TNF-α in endochondral cartilage resorption. J Bone Miner Res 2003;18(9):1584–1592. [PubMed: 12968667]
14. Gerstenfeld LC, Cho TJ, Kon T, Aizawa T, Cruceta J, Graves BD, et al. Impaired intramembranous bone formation during bone repair in the absence of tumor necrosis factor-alpha signaling. Cells Tissues Organs 2001;169(3):285–294. [PubMed: 11455125]
15. Jaiswal N, Haynesworth SE, Caplan AI, Bruder SP. Osteogenic differentiation of purified, culture-expanded human mesenchymal stem cells in vitro. J Cell Biochem 1997;64:295–312. [PubMed: 9027589]
16. Peter SJ, Liang CR, Kim DJ, Widmer MS, Mikos AG. Osteoblastic phenotype of rat marrow stromal cells cultured in the presence of dexamethasone, beta-glycerolphosphate, and L-ascorbic acid. J Cell Biochem 1998;71:55–62. [PubMed: 9736454]
17. Datta N, Holtorf HL, Sikavitsas VI, Jansen JA, Mikos AG. Effect of bone extracellular matrix synthesized in vitro on the osteoblastic differentiation of marrow stromal cells. Biomaterials 2005;26 (9):971–977. [PubMed: 15369685]

18. Rhen T, Cidlowski JA. Antiinflammatory action of glucocorticoids--new mechanisms for old drugs. N Engl J Med 2005;353(16):1711–1723. [PubMed: 16236742]
19. Balga R, Wetterwald A, Portenier J, Dolder S, Mueller C, Hofstetter W. Tumor necrosis factor-alpha: Alternative role as an inhibitor of osteoclast formation in vitro. Bone 2006;39(2):325–335. [PubMed: 16580896]
20. Datta N, Pham QP, Sharma U, Sikavitsas VI, Jansen JA, Mikos AG. In vitro generated extracellular matrix and fluid shear stress synergistically enhance 3D osteoblastic differentiation. Proc Natl Acad Sci U S A 2006 Feb 21;103(8):2488–2493. [PubMed: 16477044]
21. Pham QP, Sharma U, Mikos AG. Electrospinning of polymeric nanofibers for tissue engineering applications: a review. Tissue Eng 2006;12(5):1197–1211. [PubMed: 16771634]
22. Pham QP, Sharma U, Mikos AG. Electrospun poly(epsilon-caprolactone) microfiber and multilayer nanofiber/microfiber scaffolds: characterization of scaffolds and measurement of cellular infiltration. Biomacromolecules 2006;7(10):2796–2805. [PubMed: 17025355]
23. Gomes ME, Bossano CM, Johnston CM, Reis RL, Mikos AG. In vitro localization of bone growth factors in constructs of biodegradable scaffolds seeded with marrow stromal cells and cultured in a flow perfusion bioreactor. Tissue Eng 2006;12(1):177–188. [PubMed: 16499454]
24. Gomes ME, Holtorf HL, Reis RL, Mikos AG. Influence of the porosity of starch-based fiber mesh scaffolds on the proliferation and osteogenic differentiation of bone marrow stromal cells cultured in a flow perfusion bioreactor. Tissue Eng 2006;12(4):801–809. [PubMed: 16674293]
25. Martins AM, Pham QP, Malafaya PB, Sousa RA, Gomes ME, Raphael RM, et al. The role of lipase and a-amylase in both the degradation of starch/poly(e-caprolactone) fiber meshes and the osteogenic differentiation of cultured marrow stromal cells. Tissue Eng Part A 2009;15(2):295–305. [PubMed: 18721077]
26. Prockop DJ. Marrow stromal cells as stem cells for nonhematopoietic tissues. Science 1997;276 (5309):71–74. [PubMed: 9082988]
27. Lewis M, Tartaglia LA, Lee A, Bennett GL, Rice GC, Wong GH, et al. Cloning and expression of cDNAs for two distinct murine tumor necrosis factor receptors demonstrate one receptor is species specific. Proc Natl Acad Sci U S A 1991;88(7):2830–2834. [PubMed: 1849278]
28. Merchant, FA.; Periasamy, A. Correction Using Calibration Images. In: Wu, Q.; Merchant, FA.; Castleman, KR., editors. Microscope Image Processing. Burlington; Elsevier: 2008. p. 258
29. Pape H-C, Schmidt RE, Rice J, van Griensven M, das Gupta R, Krettek C, et al. Biochemical changes after trauma and skeletal surgery of the lower extremity: Quantification of the operative burden. Crit Care Med 2000;28(10):3441–3448. [PubMed: 11057799]
30. Iqbal J, Sun L, Kumar TR, Blair HC, Zaidi M. Follicle-stimulating hormone stimulates TNF production from immune cells to enhance osteoblast and osteoclast formation. Proc Natl Acad Sci U S A 2006;103(40):14925–14930. [PubMed: 17003115]
31. Young S, Patel ZS, Kretlow JD, Murphy MB, Mountziaris PM, Baggett LS, et al. Dose effect of dual delivery of vascular endothelial growth factor and bone morphogenetic protein-2 on bone regeneration in a rat critical-size defect model. Tissue Eng Part A 2009;15:2347–2362. [PubMed: 19249918]
32. Gilbert L, He X, Farmer P, Boden S, Kozlowski M, Rubin J, et al. Inhibition of osteoblast differentiation by tumor necrosis factor-alpha. Endocrinology 2000;141(11):3956–3964. [PubMed: 11089525]
33. Taichman RS, Hauschka PV. Effects of interleukin-1β and tumor necrosis factor-α on osteoblastic expression of osteocalcin and mineralized extracellular matrix in vitro. Inflammation 1992;16(6): 587–601. [PubMed: 1459694]
34. Gilbert LC, Rubin J, Nanes MS. The p55 TNF receptor mediates TNF inhibition of osteoblast differentiation independently of apoptosis. Am J Physiol Endocrinol Metab 2005;288(5):E1011–1018. [PubMed: 15625085]
35. Castano-Izquierdo H, Alvarez-Barreto J, van den Dolder J, Jansen JA, Mikos AG, Sikavitsas VI. Pre-culture period of mesenchymal stem cells in osteogenic media influences their in vivo bone forming potential. J Biomed Mater Res A 2007;82(1):129–138. [PubMed: 17269144]
36. Paula-Silva FWG, Ghosh A, Silva LAB, Kapila YL. TNF-{alpha} Promotes an Odontoblastic Phenotype in Dental Pulp Cells. J Dent Res 2009;88(4):339–344. [PubMed: 19407154]

37. Tintut Y, Patel J, Parhami F, Demer LL. Tumor Necrosis Factor-{alpha} Promotes In Vitro Calcification of Vascular Cells via the cAMP Pathway. Circulation 2000;102(21):2636–2642. [PubMed: 11085968]

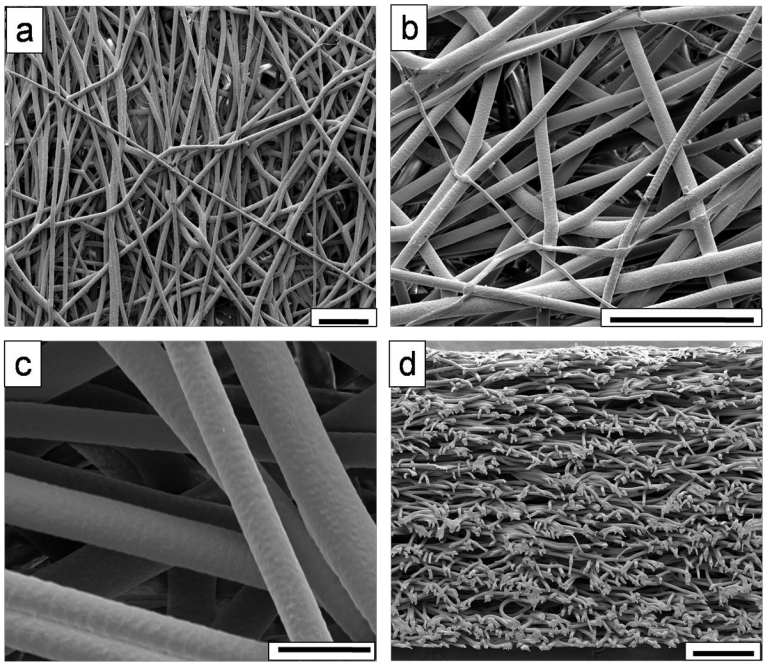

Figure 1.
Electrospun microfibers generated for this study, imaged via SEM at varying magnifications, (a) 200×, (b) 600×, and (c) 2000×. A cross-section through the entire thickness of a representative scaffold is shown in (d), at 120× magnification. Scale bars shown for (a) and (b) represent 100 μm, 20 μm for (c), and 200 μm for (d).

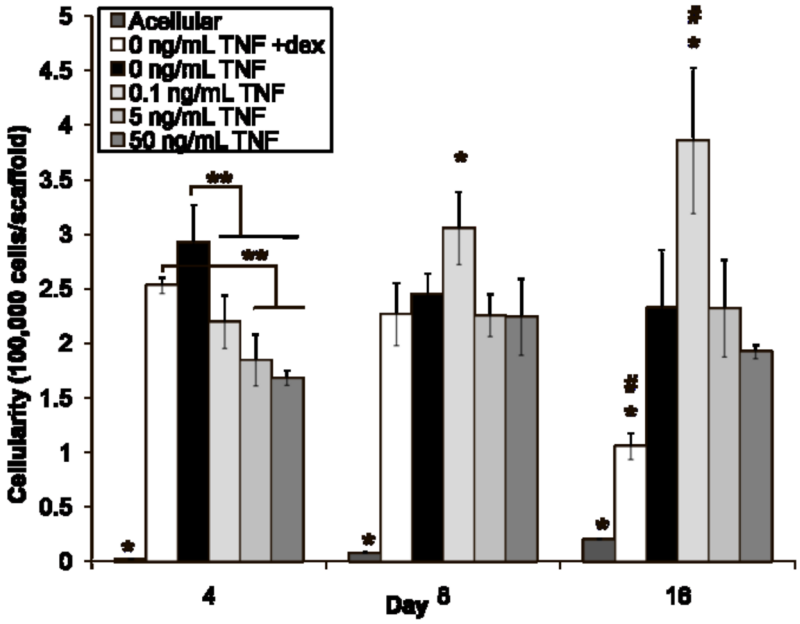

Figure 2.

Cellularity of MSC-seeded electrospun PCL scaffolds after 4, 8, and 16 days of culture. Three freeze/thaw/sonication cycles were used to extract dsDNA, which was then quantified with a fluorometric kit and translated to cells/scaffold. Experimental groups were cultured in dexamethasone-free osteogenic media supplemented with 0.1, 5, or 50 ng/mL TNF-α (abbreviated "TNF" in the figure). Three control groups were included: a positive control supplemented with dexamethasone, but no TNF-α ("0 ng/mL TNF +dex"); a negative control cultured without any added dexamethasone ("0 ng/mL TNF"); and an acellular control, where cell-free PCL scaffolds were cultured in dexamethasone-free media ("Acellular"). Each bar represents the mean ± standard deviation for $n = 4$ constructs. Error bars are included for all groups, though they are too small to resolve for "Acellular." Statistical differences ($p < 0.05$) among groups at a single timepoint are indicated by "*" for a group that differs from all other groups, and "**" for a group that differs from only some groups. Changes over time are indicated by "#," meaning that values for that group at each timepoint are significantly different ($p < 0.05$).

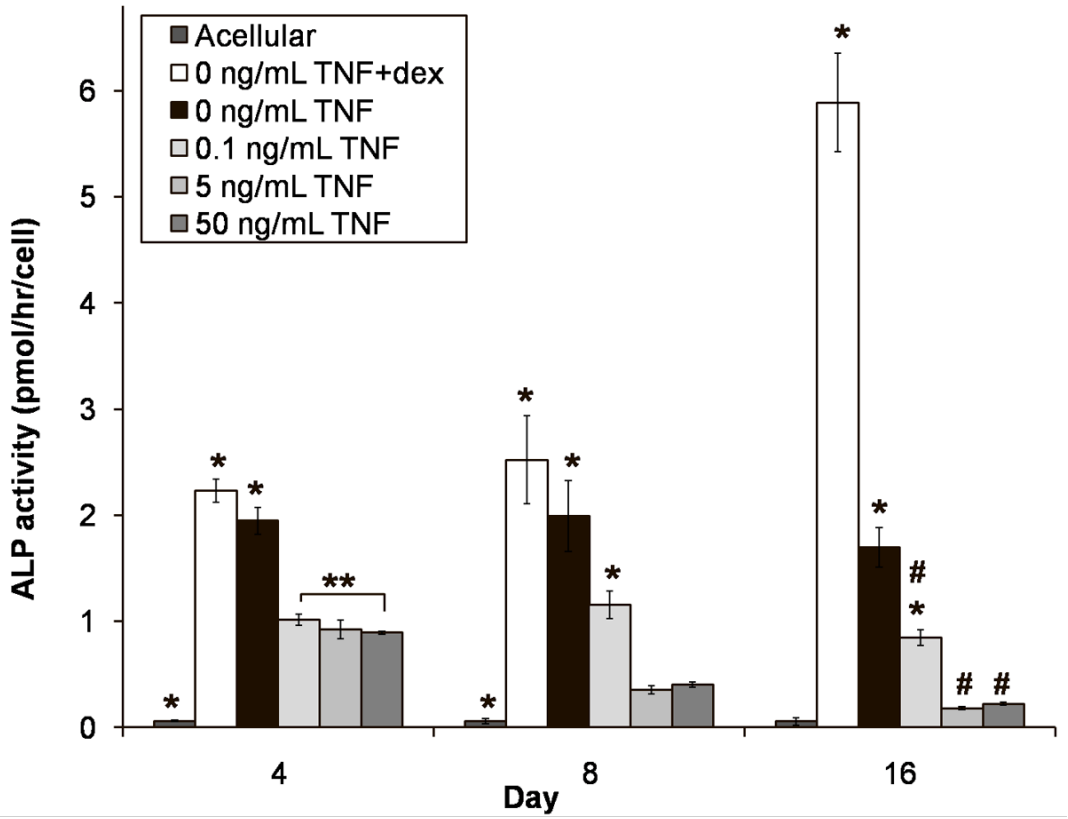

Figure 3.

Alkaline phosphatase (ALP) activity of MSC-seeded electrospun PCL scaffolds after 4, 8, and 16 days of culture. Experimental groups were cultured in dexamethasone-free osteogenic media supplemented with 0.1, 5, or 50 ng/mL TNF-α (abbreviated "TNF" in the figure). Three control groups were included: a positive control supplemented with dexamethasone, but no TNF-α ("0 ng/mL TNF +dex"); a negative control cultured without any added dexamethasone ("0 ng/mL TNF"); and an acellular control, where cell-free PCL scaffolds were cultured in dexamethasone-free media ("Acellular"). Each bar represents the mean ± standard deviation for $n = 4$ constructs. Error bars are included for all groups, though they are too small to resolve in some cases. Statistical differences ($p < 0.05$) among groups at a single timepoint are indicated by "*" for a group that differs from all other groups, and "**" for a group that differs from only some groups. Changes over time are indicated by "#," meaning that values for that group at each timepoint are significantly different ($p < 0.05$).

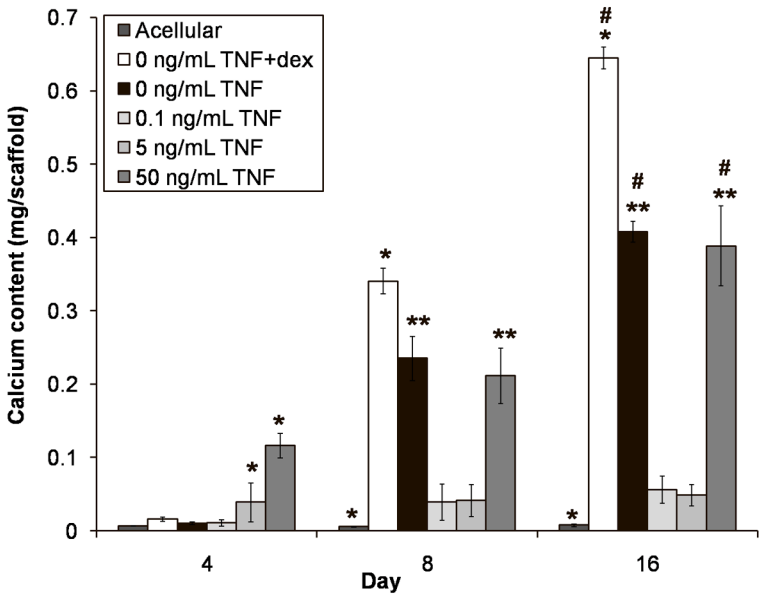

Figure 4.

Calcium content of MSC-seeded electrospun PCL scaffolds after 4, 8, and 16 days of culture. Experimental groups were cultured in dexamethasone-free osteogenic media supplemented with 0.1, 5, or 50 ng/mL TNF-α (abbreviated "TNF" in the figure). Three control groups were included: a positive control supplemented with dexamethasone, but no TNF-α ("0 ng/mL TNF +dex"); a negative control cultured without any added dexamethasone ("0 ng/mL TNF"); and an acellular control, where cell-free PCL scaffolds were cultured in dexamethasone-free media ("Acellular"). Each bar represents the mean ± standard deviation for $n = 4$ constructs. Error bars are included for all groups, though they are too small to resolve in some cases. Statistical differences ($p < 0.05$) among groups at a single timepoint are indicated by "*" for a group that differs from all other groups, and "**" for groups that do not differ from each other, but differ from all other groups. Changes over time are indicated by "#," meaning that values for that group at each timepoint are significantly different ($p < 0.05$).

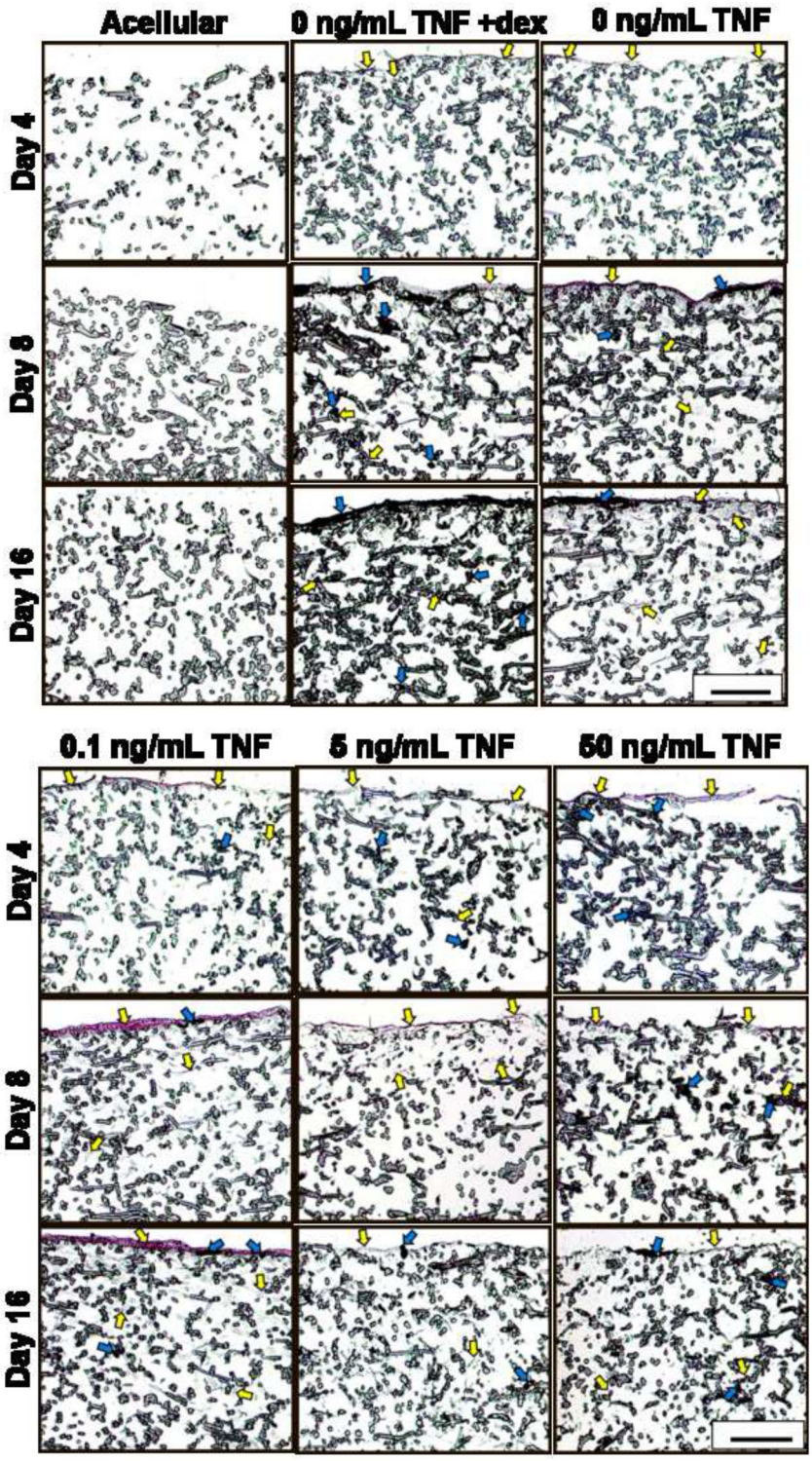

Figure 5.

Representative cross-sectional images (5 μm thick) of stained MSC-seeded electrospun PCL scaffolds after 4, 8, and 16 days of culture. Sections were stained with von Kossa and eosin. Each image shows only the top half of each cross-section, which is where cells (representative

examples indicated by yellow arrows) and mineral deposits (representative examples marked with blue arrows) were located. Experimental groups were cultured in dexamethasone-free osteogenic media supplemented with 0.1, 5, or 50 ng/mL TNF-α (abbreviated “TNF” in the figure). Three control groups were included: a positive control supplemented with dexamethasone, but no TNF-α (“0 ng/mL TNF +dex”); a negative control cultured without any added dexamethasone (“0 ng/mL TNF”); and an acellular control, where cell-free PCL scaffolds were cultured in dexamethasone-free media (“Acellular”). Images were captured at 10× original magnification. Scale bar in lower right corner represents 200 μm and applies to all images.

Table 1

Comparison of Fiber Diameters and Porosities for the Two Electrospun PCL Meshes Used for this Study[a]

Parameter for Comparison	Value for Mesh 1	Value for Mesh 2
Fiber Diameter, Top (μm)	9.50 ± 1.57	9.37 ± 2.04
Fiber Diameter, Bottom (μm)	11.58 ± 2.23	11.76 ± 1.79
Porosity (%)	77.8 ± 2.8*	79.5 ± 3.1*

[a]Values are presented as mean ± standard deviation. The sample size was N = 45 for fiber diameters from the top and bottom of each mesh, and N = 50 scaffolds for PCL mesh porosity. Pairs of values were compared and statistically significant differences ($P < 0.05$) are indicated with a "*."